Semiconductor Snail Lasers

M.J. Strain,[1, a)] G. Mezösi,[1] M. Sorel,[1] A. Pérez-Serrano,[2] A. Scirè,[2] S. Balle,[3] G. Verschaffelt,[4] and J. Danckaert[4]

[1)] *E&EE Dept., University of Glasgow, Glasgow, G12 8LT, United Kingdom*

[2)] *IFISC, UIB-CSIC, Campus UIB, E-07122 Palma de Mallorca, Spain*

[3)] *IMEDEA - C/ Miquel Marqus, 21 - 07190 Esporles - Islas Baleares, Spain*

[4)] *Dept. Applied Physics and Photonics, Vrije Universiteit Brussel, Pleinlaan 2, 1050, Brussels, Belgium*

(Dated: 1 December 2009)

A modified ring laser geometry is presented to promote stable unidirectional lasing. The effects of directional coupling and feedback strength are investigated with respect to quantum efficiency, directionality and side-mode suppression ratio of the lasing spectra. Simulation and experimental results are presented showing single mode ($> 20dB$ side-mode suppression ratio), unidirectional lasing on an InP based multiple quantum well material.

Semiconductor ring lasers (SRL) are becoming a mature and versatile technology with applications in telecommunications, optical signal processing and on-chip sensing. Research carried out into SRL devices has demonstrated many of the functions that have been previously presented in Fabry-Pérot (FP) and Distributed Feedback (DFB) lasers; such as tunability[1], master-slave operation[1] and mode-locking[2]. Additionally, directional bistability has been demonstrated[3], with possible future applications in optical memory and delay lines.

Further application of SRLs may be made in high power applications, especially where spatially dense arrays of outputs are required, for example in high resolution printing heads. SRLs possess two key advantages over FP devices in such applications. Firstly, SRLs do not suffer from the Catastrophic Optical Damage (COD) that occurs in FP lasers where the cleaved facets are employed as feedback elements in the laser cavity. In ring lasers, the lasing cavity is formed by the closed ring waveguide with light extracted using waveguide coupler structures, avoiding inclusion of facets in the lasing cavity. The second advantage this provides, is that the lasers may be spatially separated on chip, allowing better thermal management and contact definition for individual addressing, without the considerations that would be necessary for FP devices, such as waveguide bends or etched cavity mirrors. However, it is difficult to realise the equivalent to high and low reflectivity facet coatings, which allow increased quantum efficiency and directionally dependent output power, in a ring geometry. The symmetric nature of the coupling in ring lasers can produce both bidirectional or (fluctuating) bistable directional lasing of the device[4]. Unidirectionality is dependent on minimising feedback within the laser cavity, which, by coupling energy between counter-propagating modes leads to bidirectional emission. So, the necessity for high output coupling for increased quantum efficiency of ring lasers also results in increased feedback into the laser cavity and hence, bidirectional lasing. In this paper an alternative 'snail' ring laser geometry is presented as a means to produce high efficiency, stable unidirectional lasing.

Fig. 1 shows a schematic of the snail laser device. The laser has one cleaved output facet, and the input waveguide is curved until it couples with itself, forming a ring cavity. The waveguide is then terminated inside the ring with a second, etched, facet. This laser geometry

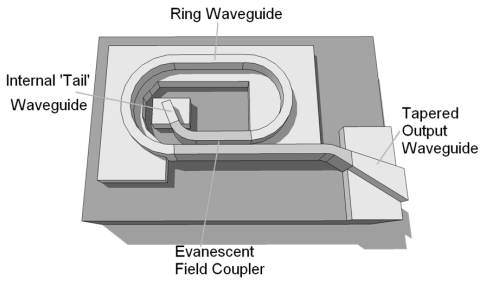

FIG. 1. Schematic of a snail laser device.

is proposed with two objectives in mind. Firstly, lasers with highly directional output are required, something achieved in FP devices using facet coatings. In ring laser geometries directionality is achieved by lasing on only one of the two counter propagating modes, an effect that may be achieved by applying external injection or feedback to the cavity. In the snail laser, the feedback from the two facets is unbalanced, given that the output facet is tilted and tapered in order to reduce back reflections, whilst the internal 'tail' facet is untapered and left as etched, to produce a higher reflectivity. This imbalance produces greater feedback into the counter-clockwise (CCW) mode (as defined by the schematic), so creating unidirectional lasing in this direction. Secondly, high slope efficiency is sought, i.e. a large proportion of the lasing mode in the cavity is required to be extracted. In a normal ring geometry this would entail producing a directional coupler (DC) with a high coupling fraction, in other words, a high percentage of the modal power must be out-coupled each

[a)] mstrain@elec.gla.ac.uk

roundtrip. Producing DCs with large coupling fractions on semiconductor devices requires a compromise between small gaps separating the co-propagating waveguides (requiring highly optimised pattern definition and etching) and coupler lengths (leading to device lengths in the order of hundreds of microns.) By using the snail geometry this problem is inverted, and rather than having to out-couple large proportions of light each roundtrip, the cavity geometry requires low coupling back into the ring each roundtrip. This requirement for low coupling DCs, reduces the fabrication tolerances significantly, allowing the production of short, widely spaced co-propagating waveguides.

The lasing threshold current and LI behaviour as a function of the ring self-coupling coefficient (δ) - where $\delta = 0$ is equivalent to a FP cavity and $\delta = 1$ equates to a ring cavity with no out-coupling - and the facet reflectivities, were calculated using the travelling wave model[5]. Fig. 2 shows the simulated LI curves given the facet reflectivities calculated with the Finite Difference Time Domain (FDTD) method, and varying self-coupling. The inset to Fig. 2 shows a schematic of the snail laser used for simulation. The travelling wave model shows an inverse relationship between the self-coupling and both the threshold current and slope efficiency. Unidirectionality is also predicted for all of the devices. In addition, it can be noted that the self-coupling modulates the lasing cavity between a pure ring and pure FP type resonator, with intermediate values modelling an effective coupled cavity system. By solving for the allowed cavity modes of the snail geometry, that may be considered as a ring with two external cavities, the mode solutions may be obtained as a function of the ring self-coupling and the facet reflectivities and external cavity lengths. This coupled cavity effect may be expressed as a loss modulation on the allowed modes as in (1).

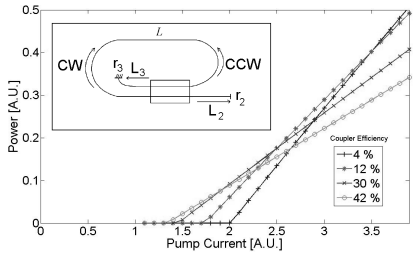

FIG. 2. Travelling Wave Model simulation of LI curves for varying self-coupling in a snail laser device.

$$\Delta Im\left(q_m^{\pm}\right) = 2\frac{1-\delta^2}{\delta L}\sqrt{r_3 r_2}cos\left(\frac{q_3 L_3 + q_2 L_2}{2}\right) \quad (1)$$

Where r_3 and r_2 are the tail and output facet reflectivities, $q_3 L_3$ and $q_2 L_2$ are the effective wavelength dependent optical lengths of the tail and output waveguides, and L is the length of the ring. From (1), as the self-coupling increases, and the cavity becomes more 'ring-like', the amplitude of the loss modulation is dominated by $[(1-\delta^2) \rightarrow 0]$ and predicts reduced coupled cavity effects. Inversely, as the self-coupling is reduced, the reflectivities of the facets dominate the modal loss modulation, predicting coupled cavity modal spectra, the amplitude modulation of which increases with increasing facet reflectivity. Therefore, in order to produce a high output laser source with high side-mode suppression, low self-coupling is required with small output facet reflectivity to maximise side-mode suppression ratio (SMSR).

In all of the designs presented here, the waveguide width is $2\,\mu m$, the output waveguide was tapered up to $8\,\mu m$ and the device bar facet cleaved at 80^o to the waveguide normal in order to minimise backreflections. The average ring radius around the snail cavity is $200\,\mu m$. The length of the output waveguides is $450\,\mu m$ and the tail waveguides are $208\,\mu m$ long. FDTD simulations of the structures gave values of 6.1% and 0.67% respectively, for the tail and output facet reflectivities at transparency. Three device variations were fabricated, modifying the length of the coupler section. The coupler lengths were $56.4, 80.5$ and $171\,\mu m$ giving nominal coupling of $5, 10$ and 40% respectively.

The devices were fabricated on a multiquantum-well (QW) InAlGaAs/InP wafer structure with a gain region consisting of five $6\,nm$ compressively strained InAlGaAs wells and six $10\,nm$ slightly tensile strained barriers. The waveguiding core is formed by a $60\,nm$ graded-index layer on either side of the QW region. Hydrogen silsesquioxane (HSQ) was used as a negative tone electron beam resist for definition of the waveguides. After exposure and development the HSQ pattern was used as a hard-mask for the etching of the uppercladding layers using a $CH_4/H_2/O_2$ Reactive Ion Etch (RIE).

Experimental LI curves for the lasers were measured by varying the main, continuous pumping current of the ring and coupling the output from the cleaved facet waveguide to a broad area Germanium photodetector. Fig. 3 shows LI curves for the snail laser devices with the tail contact biased at $0\,V$. In the figure inset, for a simple SRL, the unidirectional switching regime as described by Sorel et al.[4], can clearly be seen as the LI curve measured from

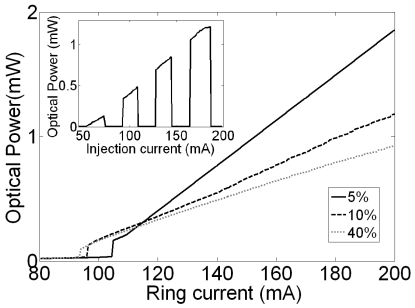

FIG. 3. LI curves for snail laser devices with varying self-coupling.(Inset: LI curve from a SRL device.)

one facet shows extinction of the mode as it switches lasing direction. The snail laser devices, as predicted by the simulation results, show increasing threshold current and quantum efficiency as a decreasing function of self-coupling. The abrupt step in power at the lasing thresholds is due to the fact that the DC sections are unpumped, creating an absorbing section in the cavity. In the snail laser LI curves there is no evidence of the switching apparent in the simple ring laser. Photocurrent measurements of the tail waveguide contact confirmed unidirectional operation. Finally, directional switching could be observed for the 40% coupled snail laser for reverse bias $< -2\,V$ on the tail contact, suggesting that as the effective reflectivity of the tail facet approaches that of the output facet, the laser is not forced to operate unidirectionally in the CCW direction.

Spectra of the snail laser devices under varying injection current, and reverse bias on the tail waveguide contact, were obtained by coupling the output facet light into a lensed single-mode fibre and an optical spectrum analyser. Fig. 4(a) exhibits the SMSR of the lasers at 2x threshold current for varying reverse bias on the tail waveguide contact. Again, these results are

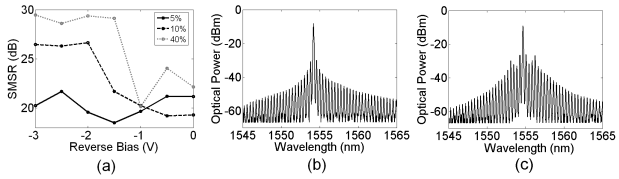

FIG. 4. (a) SMSR vs reverse bias on internal waveguide for snail lasers with varying self-coupling, (b) spectra for snail laser with 10% coupler and $-3\,V$ (b) $0\,V$ reverse bias on internal waveguide.

predicted by simulation. This effect is highlighted in Fig.4(a), where for a reverse bias of $-3\,V$ - and hence low reflectivity of r_3 - the SMSR is largest for the device with highest self-coupling. In the case of low self-coupling and significant facet reflectivities (i.e. low values of reverse bias in Fig. 4(a)), the coupled cavity effects become apparent as the system tends more to a 'ring plus external cavity' condition. For the 5% coupler device, the SMSR does not vary greatly with tail facet reflectivity, as the loss modulation term is dominated by the coupling factor. These effects are also exhibited in the experimental lasing spectra of the 10% self-coupled device shown in Fig. 4(b) and (c). The coupled cavity effect can be clearly identified in Fig. 4(c) as opposed to the single ring mode spectra of Fig. 4(b), where the increased reverse bias on the tail contact reduces its reflectivity, leading to closer to ring-like behaviour. The coupled cavity effect presents more strongly, as predicted, with decreasing coupling coefficient of the snail lasers. Finally, in order to demonstrate potential of creating dense arrays of these devices on a single chip, a set of four devices were fabricated as shown in Fig. 5, with an output waveguide pitch of $32\,\mu m$. A near field

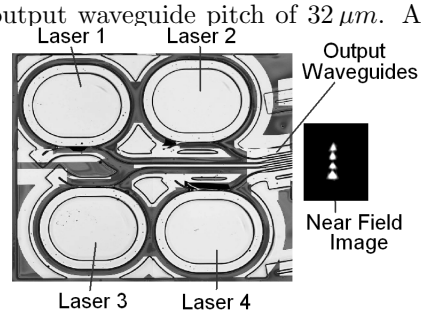

FIG. 5. Micrograph of snail laser array, with near field image of emission from four output waveguides.

image is also shown, exhibiting the four distinct output spots of the devices, each of which was individually addressable.

In conclusion, a modification of a ring laser geometry has been presented in order to produce unidirectional lasing in ring cavities. SMSRs of over $20\,dB$ were exhibited for all of the devices fabricated, with increased quantum efficiency being exhibited with reducing self-couplig. The effect of feedback from the internal waveguide was found to promote unidirectionality, but also for increasing effective reflectivity - manifested by modulating the reverse bias on the internal waveguide - coupled cavity effects were seen to emerge, reducing the SMSR, especially for devices with small coupling coefficients. Good agreement was achieved between the experimental results and simulations carried out using the travelling wave model, for the threshold, slope efficiency and SMSR behaviour of the devices. An array of four $32\,\mu m$ output pitched, individually addressable snail lasers was also presented. The snail laser has the potential to provide a high efficiency, unidirectional laser source without suffering from the COD problems associated FP laser devices where external facets form the laser feedback mechanism.

We acknowledge financial support from the IOLOS (034743) project funded by the European Unions Sixth Framework Program (EU FP6-2005-IST-5). The authors would like to thank J. Javaloyes, D. Yanson, M. Silver, the staff of the JWNC and B. Ward.

[1]S. Furst, S. Yu, and M. Sorel, IEEE Photon. Technol. Lett. **20**, 1926–1928 (2008).
[2]Y. Barbarin, E. A. J. M. Bente, M. J. R. Heck, Y. S. Oei, R. Notzel, and M. K. Smit, Optics Expr. **14**, 9716–9727 (2006).
[3]M. Hill, Nature **432**, 206 (2004).
[4]M. Sorel, G. Giuliani, A. Scire, R. Miglierina, S. Donati, and P. Laybourn, IEEE J. Quantum Electron. **39**, 1187–1195 (2003).
[5]J. Javaloyes and S. Balle, IEEE J. Quantum Electron. **45**, 431–438 (2009).